Role of ERO1-α–mediated stimulation of inositol 1,4,5-triphosphate receptor activity in endoplasmic reticulum stress–induced apoptosis

Gang Li,[1] Marco Mongillo,[2,4] King-Tung Chin,[5] Heather Harding,[5] David Ron,[5] Andrew R. Marks,[2,4] and Ira Tabas[1,2,3,4]

[1]Department of Medicine, [2]Department of Physiology and Cellular Biophysics, [3]Department of Pathology and Cell Biology, and [4]Clyde and Helen Wu Center for Molecular Cardiology, Columbia University, New York, NY 10032
[5]Helen L. and Martin S. Kimmel Center for Biology and Medicine, Skirball Institute of Biomolecular Medicine, New York University School of Medicine, New York, NY 10016

Endoplasmic reticulum (ER) stress–induced apoptosis is involved in many diseases, but the mechanisms linking ER stress to apoptosis are incompletely understood. Based on roles for C/EPB homologous protein (CHOP) and ER calcium release in apoptosis, we hypothesized that apoptosis involves the activation of inositol 1,4,5-triphosphate (IP3) receptor (IP3R) via CHOP-induced ERO1-α (ER oxidase 1 α). In ER-stressed cells, ERO1-α is induced by CHOP, and small interfering RNA (siRNA) knockdown of ERO1-α suppresses apoptosis. IP3-induced calcium release (IICR) is increased during ER stress, and this response is blocked by siRNA-mediated silencing of ERO1-α or IP3R1 and by loss-of-function mutations in *Ero1a* or *Chop*. Reconstitution of ERO1-α in *Chop*$^{-/-}$ macrophages restores ER stress–induced IICR and apoptosis. In vivo, macrophages from wild-type mice but not *Chop*$^{-/-}$ mice have elevated IICR when the animals are challenged with the ER stressor tunicamycin. Macrophages from insulin-resistant *ob/ob* mice, another model of ER stress, also have elevated IICR. These data shed new light on how the CHOP pathway of apoptosis triggers calcium-dependent apoptosis through an ERO1-α–IP3R pathway.

Introduction

Cells possess an important set of integrated signal transduction pathways to ensure proper functioning of the ER under conditions of ER stress or disequilibrium (Malhotra and Kaufman, 2007). However, in certain pathophysiologic situations such as neurodegenerative disease, diabetes, and atherosclerosis, ER stress and ER stress signaling through the unfolded protein response (UPR) are prolonged, leading to apoptosis (Kim et al., 2008). Although activation of apoptosis pathways involving IRE1-α or caspase-12 appears to be applicable to a limited number of ER stress scenarios (Nakagawa et al., 2000; Nishitoh et al., 2002), apoptosis involving the distal UPR-induced transcription factor C/EPB homologous protein (CHOP; GADD153; DDIT3) has been implicated in a wide variety of pathological conditions (Zinszner et al., 1998; Oyadomari et al., 2002; Tajiri et al., 2006; Kim et al., 2008; Song et al., 2008; Thorp et al., 2009). Remarkably, much remains to be learned about the molecular mechanisms linking CHOP expression to specific apoptotic processes. Previous studies have shown that CHOP can suppress prosurvival molecules like Bcl-2 and Trb3 and induce proapoptotic BIM (Bcl-2–interacting mediator of cell death) and oxidant stress (Puthalakath et al., 2007; Kim et al., 2008; Song et al., 2008). However, the precise mechanisms linking these processes to cell death are uncertain.

As a pathophysiologically relevant model of ER stress/CHOP-induced apoptosis, our laboratory has been studying UPR-induced macrophage apoptosis (Feng et al., 2003; Kim et al., 2008). This process depends on CHOP and plays an important role in plaque necrosis in advanced atherosclerosis (Feng et al., 2003; Thorp et al., 2009). In this model, ER-released cytosolic calcium plays a critical role in the activation

Correspondence to Ira Tabas: iat1@columbia.edu

Abbreviations used in this paper: AUC, area under the curve; CHOP, C/EPB homologous protein; IICR, IP3-induced calcium release; IP3, inositol 1,4,5-triphosphate; IP3R, IP3 receptor; MEF, murine embryonic fibroblast; NAC, *N*-acetyl-Cys; PERK, PKR-like ER kinase; RT-QPCR, reverse transcriptase quantitative PCR; SERCA, sarcoplasmic/ER calcium ATPase; UPR, unfolded protein response; WT, wild type.

The Rockefeller University Press $30.00
J. Cell Biol. Vol. 186 No. 6 783–792
www.jcb.org/cgi/doi/10.1083/jcb.200904060

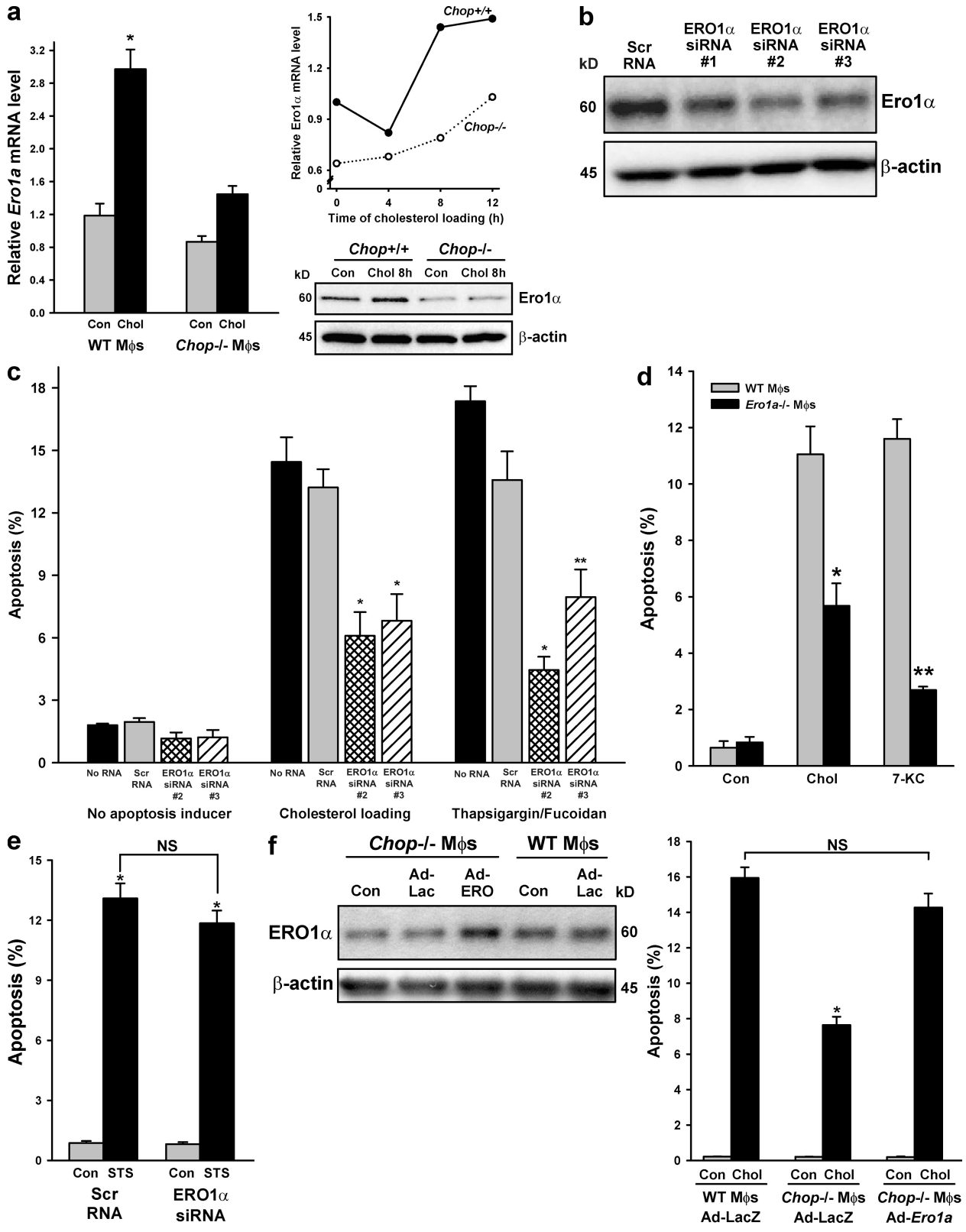

Figure 1. **Role of ERO1-α in ER stress–induced apoptosis in macrophages.** (a) Macrophages from *Chop*$^{+/+}$ (WT) and *Chop*$^{-/-}$ mice were incubated under control (Con) or cholesterol-loading (Chol) conditions for 8 h. *Ero1a* mRNA was then assayed by RT-QPCR (left; *, $P < 0.001$ for *Ero1a* mRNA). The graph on the top right shows the time course for this response; data points represent the mean of duplicate samples, which varied by <10% from each other. The immunoblot shows the ERO1-α protein level at 8 h. (b) Macrophages were transfected with three separate siRNA species directed against murine *Ero1a*. 72 h after transfection, ERO1-α protein was assayed by immunoblotting. (c) Macrophages were incubated for 30 h under control conditions, under cholesterol-loading conditions, or with 0.25 μM thapsigargin plus 25 μg/ml of the type A scavenger receptor ligand fucoidan. In each of these three groups of cells, there were four pretreatment subgroups: no RNA, scrambled (Scr) RNA, ERO1-α siRNA #2, or ERO1-α siRNA #3. At the end of the 30-h incubation, the cells were analyzed for apoptosis by annexin V staining (*, $P < 0.01$; and **, $P < 0.05$ vs. other values in same group). (d) Macrophages from

of several death effector pathways downstream of the calcium-activated signaling kinase CaMKII (Seimon et al., 2006; Lim et al., 2008; Timmins et al., 2009). Thus, in ER-stressed macrophages, as in many other scenarios involving ER stress–induced and calcium-mediated apoptosis (Kim et al., 2008), a key goal is to elucidate the molecular antecedents of ER calcium release. Based on a previous study showing the ability of the CHOP target ERO1-α (ER oxidase 1 α) to hyperoxidize the lumen of the ER (Marciniak et al., 2004) and another suggesting oxidation-induced activation of the ER calcium release channel inositol 1,4,5-triphosphate (IP3) receptor (IP3R; Higo et al., 2005), we set out to test the novel hypothesis that CHOP, through ERO1-α induction, activates IP3R-mediated ER calcium release and thereby triggers apoptosis.

Results and discussion

ERO1-α is critical for ER stress–induced apoptosis

UPR-induced apoptosis can be triggered by a robust ER stress stimulus or through the combination of low level ER stress plus a "second hit" (Zinszner et al., 1998; Seimon and Tabas, 2009). In macrophages, the former mechanism can be modeled using tunicamycin, azetidine, or 7-ketocholesterol, an athero-relevant UPR activator. The two-hit mechanism can be modeled by (a) excess lipoprotein–cholesterol, in which the ER stress stimulus is cholesterol loading of the ER membrane and the second hit is lipoprotein-mediated engagement of pattern recognition receptors, which enhance ER stress–induced apoptotic pathways and suppress compensatory cell survival pathways (Feng et al., 2003; Li et al., 2004; DeVries-Seimon et al., 2005; Seimon et al., 2006; Thorp et al., 2009); or (b) the combination of low dose thapsigargin as the ER stressor and fucoidan, a ligand for the type A scavenger receptor, as the second hit (DeVries-Seimon et al., 2005). Using the lipoprotein–cholesterol model, we found an approximately twofold increase in *Ero1a* mRNA and an ∼50% increase in ERO1-α protein (Fig. 1 a). In *Chop*$^{-/-}$ macrophages, the increase in *Ero1a* mRNA and both basal and ER stress–induced ERO1-α protein were diminished. Using siRNA species that decrease ERO1-α protein (Fig. 1 b) and activity (not depicted), we found that partial silencing of the oxidase led to a significant reduction in macrophage apoptosis in both the lipoprotein–cholesterol and the thapsigargin–fucoidan models (Fig. 1 c). Similar results, including those using 7-ketocholesterol, were obtained using macrophages from *Ero1a*$^{-/-}$ mice, which have no detectable ERO1-α by immunoblotting (Fig. 1 d and see Fig. 3 g). ERO1-α siRNA did not block apoptosis in macrophages treated with staurosporine, a protein kinase C inhibitor which induces apoptosis by a non-ER stress mechanism (Fig. 1 e). To further prove the role of ERO1-α in CHOP-dependent apoptosis, macrophages from wild-type (WT) or *Chop*$^{-/-}$ mice were transduced with adenovirus containing murine *Ero1a* cDNA to restore ERO1-α to a level similar to that in WT macrophages (Fig. 1 f). Cholesterol-induced apoptosis was partially suppressed in *Chop*$^{-/-}$ macrophages transduced with control adeno-LacZ, which is consistent with our previous data (Feng et al., 2003; Kim et al., 2008), but apoptosis was not suppressed in cholesterol-loaded *Chop*$^{-/-}$ macrophages transduced with *Ero1a*. These data indicate that ERO1-α plays an important role in ER stressed–induced, CHOP-dependent apoptosis in macrophages.

ERO1-α activates IP3-induced calcium release (IICR) during ER stress

Based on previous studies showing a critical role for cytosolic calcium in ER stress–induced macrophage apoptosis (Seimon et al., 2006; Lim et al., 2008) and a possible link between the redox state of the ER lumen and IP3R function (Higo et al., 2005; Kang et al., 2008), we tested the hypothesis that ERO1-α would sensitize IP3Rs to IP3-mediated activation during ER stress. Because fluorescent calcium-sensitive dyes rapidly bleach, we relied on (a) a standard assay in which IICR is acutely assessed at a given time point after ER stress using the ATP–purinergic receptor pathway as a tool to acutely generate IP3 (Charest et al., 1985) and (b) assays of IP3R-dependent, calcium-responsive processes in the cytoplasm (see next section).

When scrambled RNA–treated control macrophages were exposed to the ER stressor tunicamycin, there was an approximately twofold increase in IICR (Fig. 2 a). Note that at the time IICR was measured in these experiments, i.e., 8 h after the addition of tunicamycin, ER lumenal calcium, as assessed by recording thapsigargin-releasable calcium, was lower in the ER-stressed cells (Fig. S1 a). Therefore, the ER stress–induced increase in IICR at the time of the assay cannot be explained by higher ER lumenal calcium but rather is caused by a higher fraction of ER calcium being released via IP3R. In macrophages treated with ERO1-α siRNA, tunicamycin did not lead to an increase in IICR (Fig. 2 a), indicating that activation of IICR by tunicamycin was dependent on ERO1-α. The decrease in IICR in ERO1-α–deficient versus ERO1-α normal tunicamycin-treated cells could not be explained by a reduction in ER lumenal calcium in the ERO1-α–deficient cells (Fig. S1 a). Macrophages exposed to excess lipoprotein–cholesterol also demonstrated increased IICR, and this effect was suppressed not only by ERO1-α siRNA but also in macrophages from *Ero1a*$^{-/-}$ mice (Fig. 2, b and c). As was the case with tunicamycin, the increase in IICR with cholesterol loading cannot be explained by increased ER lumenal calcium, and the decrease in IICR with ERO1-α siRNA cannot be explained by a decrease in lumenal calcium (Fig. S1 b).

WT or *Ero1a*$^{-/-}$ mice were assayed for apoptosis after incubation for 16 h under control conditions, under cholesterol-loading conditions, or with 50 μM 7-ketocholesterol (7-KC; *, $P < 0.01$; and **, $P < 0.001$ for *Ero1a* vs. WT macrophages). (e) Macrophages were pretreated with either scrambled RNA or ERO1-α siRNA #2, incubated for 15 h in the absence (Con) or presence of 100 nM staurosporine (STS), and then analyzed for apoptosis (*, $P < 0.001$ for STS vs. control). (f) Macrophages from WT or *Chop*$^{-/-}$ mice were transduced with adenovirus (Ad) containing murine *Ero1a* cDNA or a control LacZ construct at 500 MOI. 32 h after the addition of virus, one set of cells was harvested for ERO1-α immunoblotting, and another set was incubated for 16 h under control or cholesterol-loading conditions and then assayed for apoptosis (*, $P < 0.001$). (a and c–f) Error bars show SEM ($n = 3$).

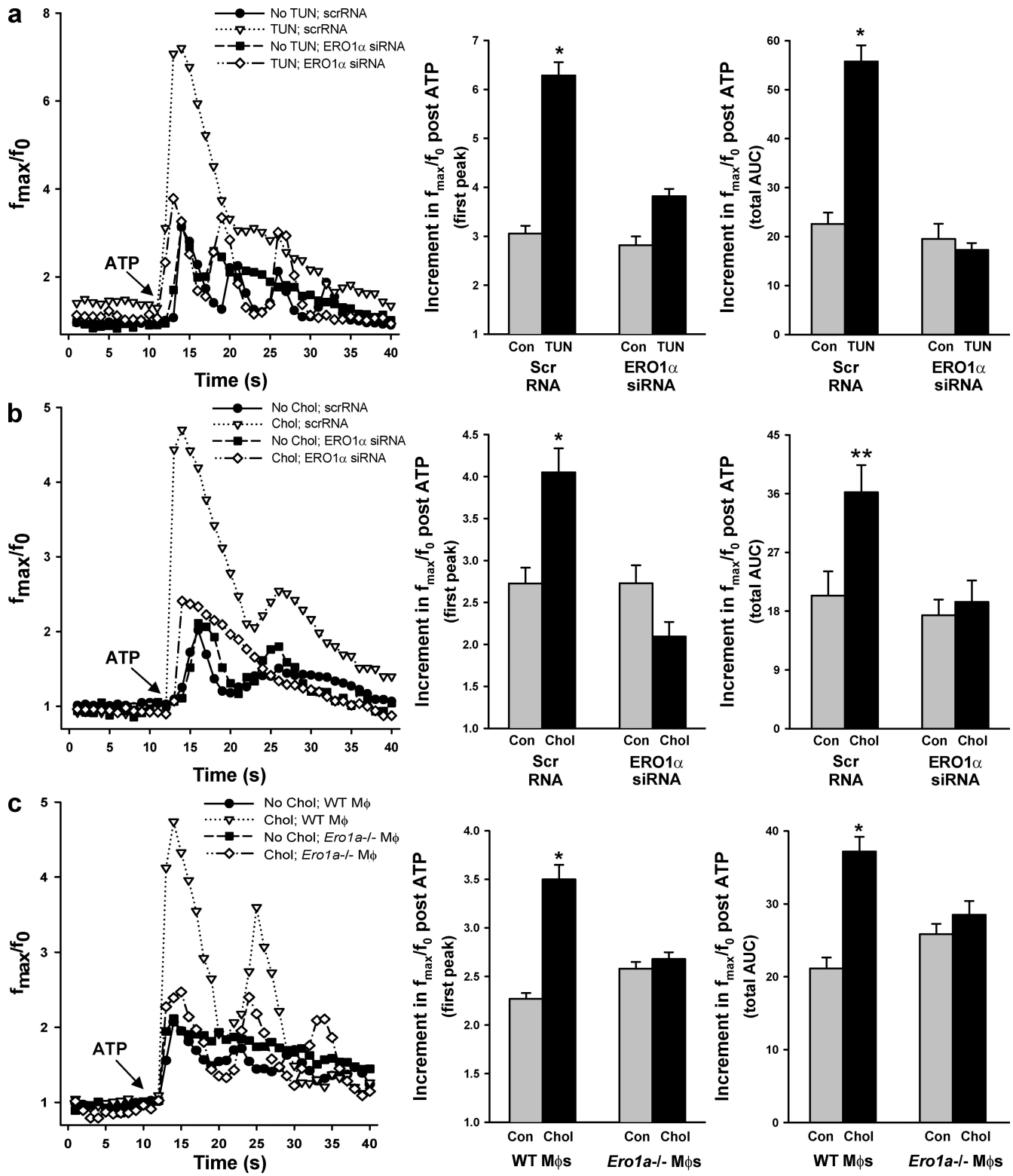

Figure 2. **Role of ERO1-α in ER stress–induced activation of IICR.** (a) Macrophages were transfected with either scrambled RNA (scrRNA) or ERO1-α siRNA, incubated for 8 h in the absence or presence of 5 µg/ml tunicamycin (TUN), and then assayed for IICR. The left graph shows a representative experiment in which Fluo-3 fluorescence is expressed as f_{max}/f_0 as a function of time (the arrow indicates ATP addition). The right bar graphs show the post-ATP area increment in f_{max}/f_0 for the first peak and AUC for the ATP-induced calcium release in the first 40 s for $n = 30$ cells (*, $P < 0.001$). (b) The experiment was conducted as in panel a, but the cells were loaded with lipoprotein–cholesterol (Chol) instead being treated with tunicamycin (*, $P < 0.01$; and **, $P < 0.05$). (c) The experiment was conducted as in panel b, but the responses in macrophages from WT or *Ero1a*$^{-/-}$ mice were compared (*, $P < 0.001$). (a–c) Error bars show SEM.

IP3R1 is necessary for ER stress–induced apoptosis

To determine directly whether IP3R is required for ER stress–induced apoptosis, we used an siRNA knockdown approach. Using reverse transcriptase quantitative PCR (RT-QPCR), we found that the major IP3R isoform expressed in macrophages is IP3R1 (unpublished data). The effect of four individual IP3R1 siRNA species on IP3R1 mRNA levels is shown in Fig. 3 a (left). The two most potent siRNAs blocked the increment in IICR in cholesterol-loaded cells (Fig. 3 a, right), and there was a close correlation between suppression of IP3R1 mRNA and suppression of cholesterol-induced apoptosis (Fig. 3 b, left). Moreover, treatment of the cells with the IP3R blocker xestospongin C (Narasimhan et al., 1998) also markedly reduced cholesterol-induced apoptosis (Fig. 3 b, right).

To determine whether these observations were applicable to another cell type, we examined murine embryonic fibroblasts (MEFs). *Ero1a*$^{-/-}$ MEFs, which have no detectable ERO1-α as measured by immunoblotting (Fig. 3 g), displayed no compensatory increase in PKR-like ER kinase (PERK) phosphorylation, CHOP expression, or XBP-1 splicing under basal conditions, and they demonstrated UPR activation after exposure to either tunicamycin or the Pro analogue azetidine to a degree similar to that in WT cells (Fig. S2). Azetidine, which promotes protein misfolding on both polysomes and free ribosomes and thus elicits both ER stress and heat shock responses (Watowich and Morimoto, 1988), caused a heightened IP3R-mediated calcium release in WT cells but not in *Ero1a*$^{-/-}$ cells (Fig. 3 c). In terms of apoptosis, both tunicamycin and azetidine triggered apoptosis, with the azetidine response being more robust, and the *Ero1a*$^{-/-}$ MEFs were protected in both situations (Fig. 3 d, left). Xestospongin C also suppressed both tunicamycin- and azetidine-induced apoptosis in MEFs (Fig. 3 d, right), indicating a role for IP3R activity. Thus, the ERO1-α–IP3R apoptosis pathway is operational in MEFs subjected to ER stress or the combination of ER stress and a heat shock response.

As mentioned previously, it is plausible that ERO1-α enhances IP3R activity by hyperoxidation of the ER lumen (Higo et al., 2005; Kang et al., 2008). Consistent with this hypothesis, the antioxidant *N*-acetyl-Cys (NAC) inhibited both the increment in IICR and apoptosis in cholesterol-loaded macrophages (Fig. 3, e and f).

Activation of CaMKII, which can be assessed by Thr287 phosphorylation, is a key signaling event linking release of ER calcium to apoptosis in ER-stressed macrophages (Lim et al., 2008; Timmins et al., 2009). Time course analyses revealed phosphorylation of the enzyme in both early and late phases of cholesterol loading, and, interestingly, it was only the later phase that required ERO1-α (Fig. 3 g). Thus, an ERO1-α–independent event may be responsible for the initial activation of CaMKII, but sustained activation of the kinase appears to be ERO1-α dependent. The data in Fig. 3 e and in Fig. S2 also show that cholesterol-induced CHOP induction is normal in *Ero1a*$^{-/-}$ macrophages. Thus, the finding that ERO1-α deletion blocks CaMKII activation and apoptosis (Fig. 1 d) under these conditions is not simply the result of reduced CHOP expression.

CHOP is necessary for activation of IICR during ER stress in vitro and in vivo

To directly link CHOP with ER calcium release, we assayed ER stress–induced, IP3R-mediated calcium release in peritoneal macrophage isolated from WT versus *Chop*$^{-/-}$ mice. In both tunicamycin-treated and cholesterol-loaded cells, we found that the increment in IICR was abrogated by *Chop* deletion (Fig. 4, a and b). Moreover, the increment in IICR could be restored in ER-stressed *Chop*$^{-/-}$ macrophages through adenovirus-mediated restoration of ERO1-α to WT levels (Fig. 4 c). Together, these findings support the existence of a CHOP–ERO1-α–IP3R pathway under conditions of ER stress.

To determine whether ER stress leads to activation of the CHOP–IP3R pathway in vivo, WT and *Chop*$^{-/-}$ mice were injected i.v. with a low dose of tunicamycin, which promotes systemic ER stress without obvious detrimental effects on the mice (Zinszner et al., 1998). Macrophages were harvested from the peritoneum and assayed soon thereafter for CHOP expression and IICR. As expected, CHOP was induced in macrophages from tunicamycin-treated WT mice (Fig. 5 a, inset). Most importantly, macrophages from WT mice but not *Chop*$^{-/-}$ mice had a significantly higher IICR than those from nontreated mice (Fig. 5 a). These data indicate that macrophage IICR is increased by systemic ER stress in vivo in a CHOP-dependent manner.

A previous study showed evidence of ER stress in the liver and adipose tissue of insulin-resistant obese mice, including leptin-deficient *ob/ob* mice (Ozcan et al., 2004), and we found that macrophages from *ob/ob* mice are more susceptible to ER stress–induced apoptosis (Senokuchi et al., 2008). Therefore, we compared macrophages from WT and *ob/ob* mice for CHOP expression and IICR. We found that macrophages freshly harvested from *ob/ob* mice had elevated expression of *Chop* mRNA and showed a striking elevation of IICR compared with macrophages from WT mice (Fig. 5, b and c). Thus, macrophage IICR is elevated in an in vivo model of insulin resistance–induced ER stress.

In summary, our data provide evidence for a new pathway linking the CHOP branch of the UPR to calcium-induced apoptosis, a scenario which has been implicated in a wide range of disease processes (Kim et al., 2008). In this sense, the mechanism revealed herein may complement another calcium-mediated apoptosis process induced by the PERK pathway that involves induction of a truncated variant of sarcoplasmic/ER calcium ATPase (SERCA) called S1T (Chami et al., 2008). The molecular mechanisms by which ERO1-α enhances IP3R activity remain to be determined. Prolonged ERO1-α induction would be expected to hyperoxidize the ER lumen (Marciniak et al., 2004), which might shift the equilibrium between the reduced and disulfide-bonded state of Cys residues in the lumenal portion of IP3R. Previous studies have correlated disulfide bond formation with activation of IP3R (Higo et al., 2005) and suggested a role for disulfide bond formation, possibly between Cys2496 and Cys2504 in IP3R1, in promoting the disruption of a repressive interaction between the protein disulfide isomerase–like protein ERp44 and IP3R (Kang et al., 2008). Our data are consistent with this concept. For example, the antioxidant NAC inhibited IICR in ER-stressed macrophages (Fig. 3 c), and

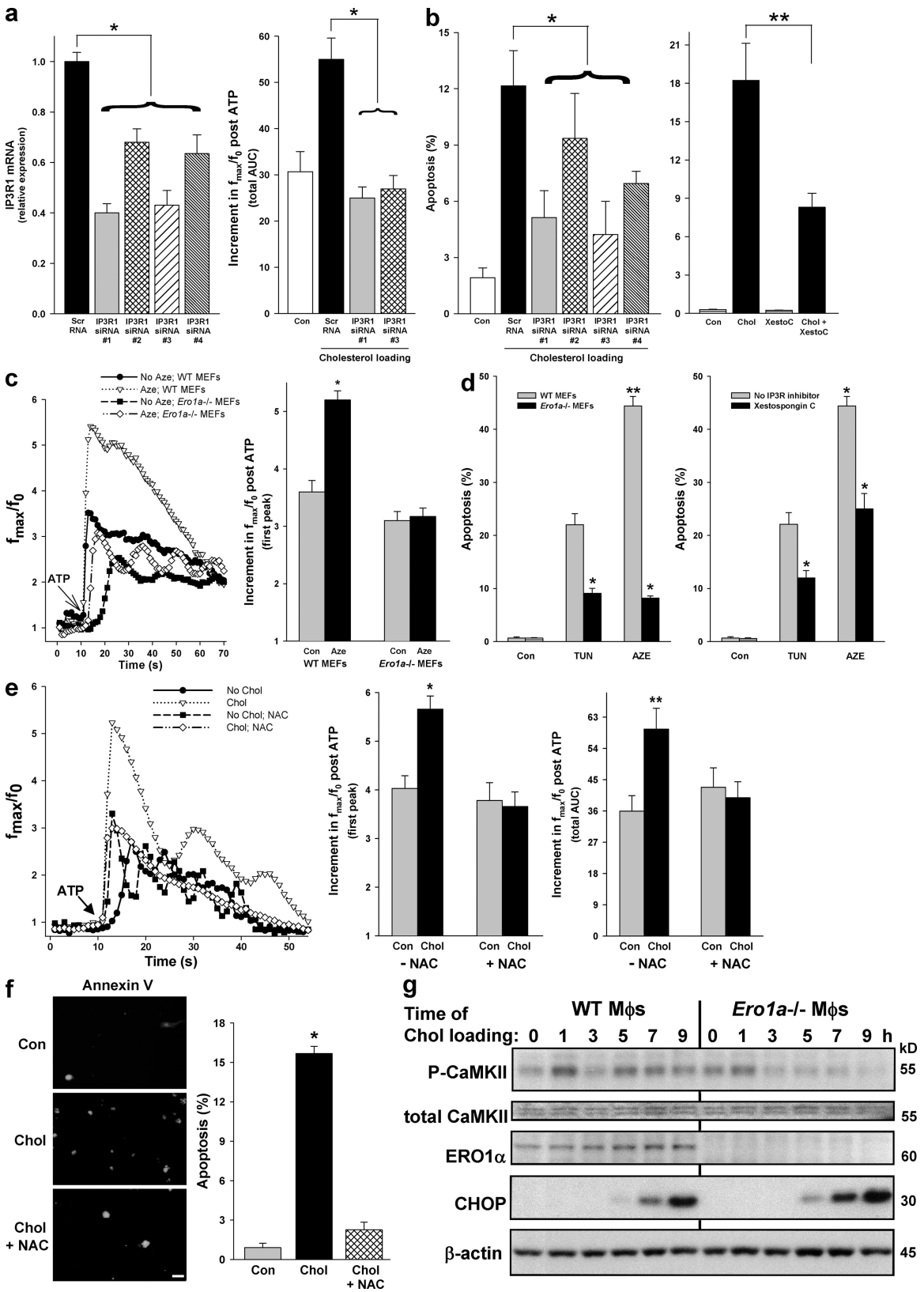

Figure 3. **Relationships among IP3R1, NAC-inhibitable oxidation, CaMKII phosphorylation, and apoptosis.** (a, left) Macrophages were transfected with four separate siRNA species directed against murine *Ip3r1*. 72 h after transfection, *Ip3r1* mRNA was assayed by RT-QPCR. (right) A separate group of cells was subjected to control (Con) or cholesterol-loading conditions and then assayed for IICR (*, $P < 0.05$). (b, left) Macrophages treated as in panel a were assayed for apoptosis by annexin V staining (*, $P < 0.05$). (right) Another group of macrophages was preincubated for 1 h with vehicle control or 0.5 μM of the IP3R inhibitor xestospongin C (XestoC), subjected to control or cholesterol-loading (Chol) conditions, also in the absence or presence of xestospongin C, and then assayed for apoptosis (**, $P < 0.01$). (c) MEFs from WT and *Ero1a*$^{-/-}$ mice were incubated for 8 h with 5 mM azetidine (Aze) and then assayed for IICR (*, $P < 0.05$). (d, left) MEFs from WT and *Ero1a*$^{-/-}$ mice were incubated for 15 h with 10 μg/ml tunicamycin (TUN) or with

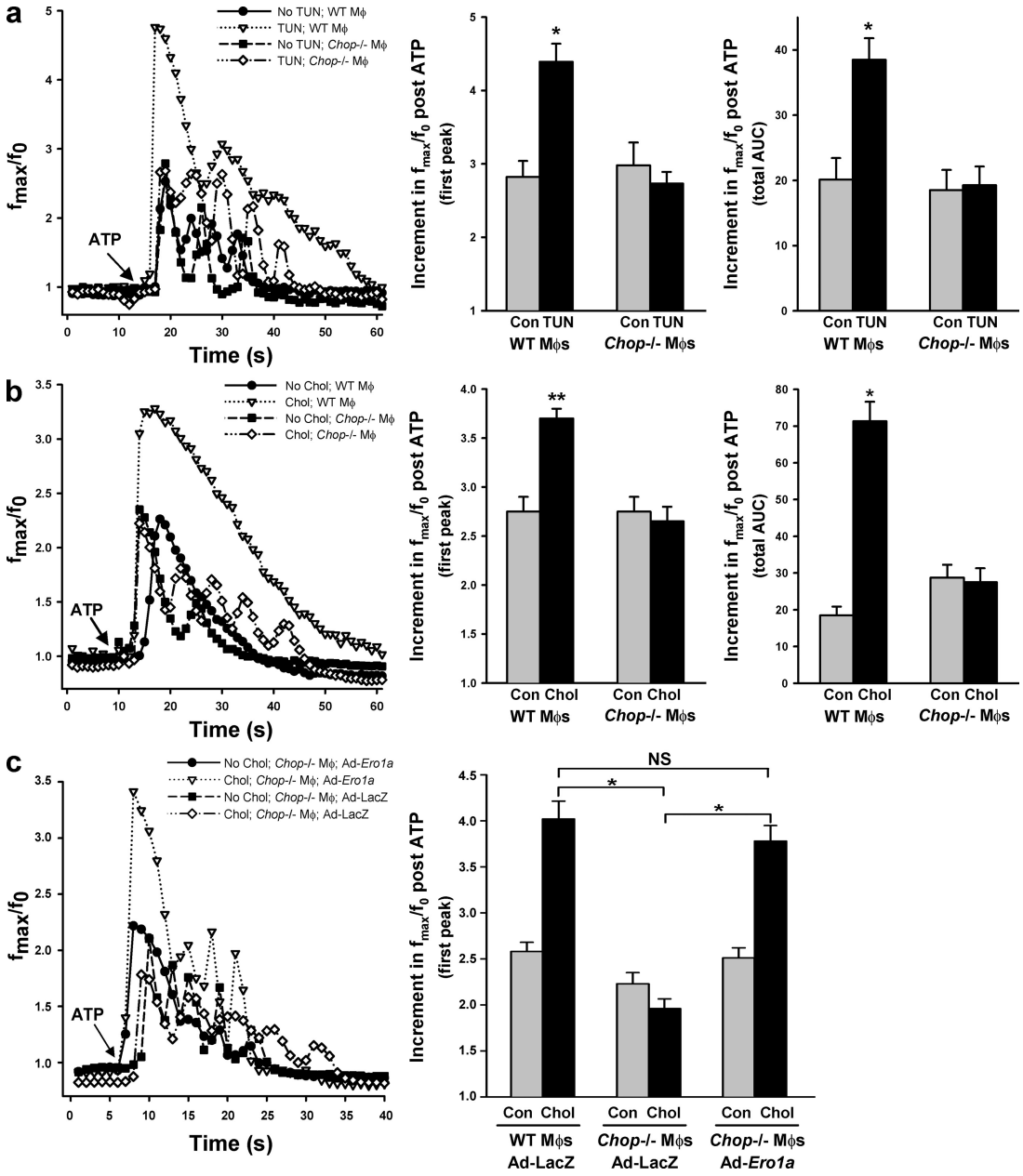

Figure 4. **Role of CHOP in ER stress–induced IICR.** (a and b) Macrophages from WT or *Chop*$^{-/-}$ mice were incubated for 8 h in the absence or presence of 5 μg/ml tunicamycin (TUN; a) or under control (Con) or cholesterol-loading (Chol) conditions (b) and then assayed for IICR (*, P < 0.001; and **, P < 0.05). (c) Macrophages from *Chop*$^{-/-}$ mice were transduced with adenovirus (Ad) containing murine *Ero1a* cDNA or a control LacZ construct at 500 MOI. 32 h after the addition of virus, the cells were assayed for IICR. Quantitative data for the post-ATP increment in first peak f_{max}/f_0, including those for control WT mice transduced with adeno-LacZ (which are not displayed on the line-scatter graph), are shown in the right graph (*, P < 0.001). The post-ATP area AUC data also showed restoration of IICR in cholesterol-loaded *Chop*$^{-/-}$ macrophages by adeno-*Ero1a* (not depicted). (a–c) Error bars show SEM (*n* = 3).

10 mM azetidine (AZE) and then assayed for apoptosis (*, P < 0.001 vs. WT MEFs; and **, P < 0.05 vs. tunicamycin group). (right) MEFs from WT mice were preincubated for 1 h with vehicle control or 0.5 μM xestospongin C, incubated for 15 h with 10 μg/ml tunicamycin or with 10 mM azetidine, also in the absence or presence of xestospongin C, and then assayed for apoptosis (*, P < 0.001 for *Ero1a*$^{-/-}$ vs. WT; for xestospongin C vs. untreated, and for azetidine vs. tunicamycin). (e) Macrophages were incubated for 8 h under control or cholesterol-loading conditions in the absence or presence of 1 mM NAC. The cells were then loaded with Fluo-3 and assayed for IICR (*, P < 0.001; and **, P < 0.05). (f) Macrophages were incubated for 16 h under control or cholesterol-loading conditions in the absence or presence of 1 mM NAC and then assayed for apoptosis. The bar graph shows the quantified data (*, P < 0.001). (a–f) Error bars show SEM (*n* = 3). (g) Macrophages from WT or *Ero1a*$^{-/-}$ mice were incubated for the indicated times under cholesterol-loading conditions. Cell lysates were then assayed by immunoblotting for expression of phospho-CaMKII (P-CaMKII), total CaMKII, ERO1-α, CHOP, and β-actin. Bar, 20 μm.

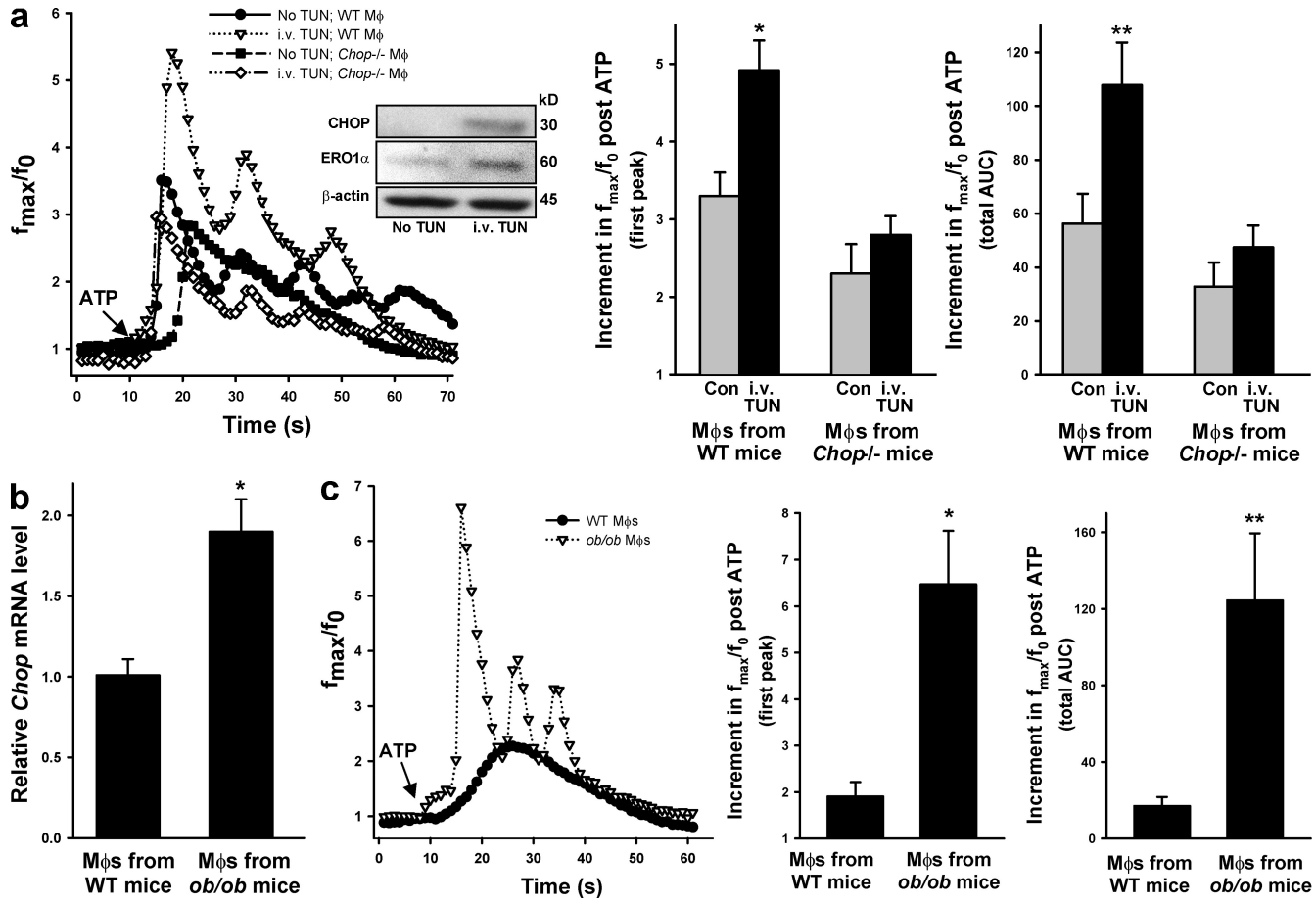

Figure 5. **ER stress–induced IICR in vivo.** (a) WT and *Chop*$^{-/-}$ mice were injected with vehicle or 0.02 mg/kg tunicamycin (TUN). 16 h later, peritoneal macrophages were harvested and assayed within 30 min for CHOP, ERO1-α, and β-actin expression by immunoblotting (inset) or for IICR (*, $P < 0.001$; **, $P < 0.05$). The arrow indicates ATP addition. (b) Macrophages from WT and *ob/ob* mice were analyzed for *Chop* mRNA by RT-QPCR (*, $P < 0.05$). (c) Macrophages from WT and *ob/ob* mice were analyzed for IICR as in panel a (*, $P < 0.01$; and **, $P < 0.05$). (a–c) Error bars show SEM ($n = 3$).

IP3R1 and ERp44 can be recovered in a complex in lysates of control macrophages but not in lysates of ER-stressed macrophages (not depicted), which correlates with low and high IICR, respectively. Moreover, the complex could also be recovered in ER-stressed macrophages in which ERO1-α was silenced by siRNA, which correlates with the suppression of IICR in these cells (unpublished data). Although the molecular details of lumenal redox regulation of IP3R activity remain to be worked out, these findings are consistent with a model in which prolonged ER stress, through ERO1-α–mediated hyperoxidation of the ER lumen, enhances IICR, at least in part, by disrupting an interaction between ERp44 and IP3R1.

A major impetus for this study was previous evidence implicating IP3R-mediated calcium release in a wide variety of apoptosis scenarios (Khan et al., 1996; Jayaraman and Marks, 1997; Deniaud et al., 2008; for review see Hajnóczky et al., 2006). In these scenarios, apoptosis often involves excess ER to mitochondria calcium flow and proapoptotic mitochondrial dysfunction, and we have shown that loss of mitochondrial membrane potential occurs and is important in ER stress–induced macrophage apoptosis (Yao and Tabas, 2001). Boehning et al. (2003) have reported that cytochrome *c*, which is released from dysfunctional mitochondria, can bind and activate IP3Rs. Thus, the IP3R–calcium–mitochondria pathway of death might be part of a positive feedback amplification cycle. In addition, several publications have reported that activation of ryanodine receptors and/or inactivation of the ER calcium ATPase pump SERCA might also contribute to calcium-induced apoptosis (for review see Hajnóczky et al., 2006). Regarding SERCA, calreticulin-mediated recruitment of ERp57 promotes the formation of an inhibitory disulfide bond (Li and Camacho, 2004). Thus, analogous redox mechanisms, one of which activates IP3R and the other of which inhibits SERCA, could promote the accumulation of cytosolic calcium by complementary mechanisms. The concept of amplification of the calcium response during apoptosis is important because physiological ER release and mitochondrial uptake of calcium must be distinct from those processes involved in apoptosis.

We have shown recently that CHOP deficiency leads to a decrease in macrophage apoptosis and plaque necrosis in advanced atheromata of fat-fed *Apoe*$^{-/-}$ and *Ldlr*$^{-/-}$ mice (Thorp et al., 2009). Moreover, we show in this study that macrophages from obese mice have increased expression of CHOP and increased ERO1-α–dependent IICR. Importantly, macrophages from obese, insulin-resistant mice are more susceptible to ER stress–induced apoptosis, and macrophage

insulin resistance promotes macrophage apoptosis and plaque necrosis in advanced atherosclerotic lesions (Han et al., 2006). The link between obesity/insulin resistance and ER stress–induced macrophage apoptosis is a critical point because the epidemic of obesity and insulin resistance is becoming the major driver of cardiovascular disease in industrialized societies (Grundy, 2004). The new mechanistic insights described in this study may suggest novel strategies to prevent pathophysiologic ER stress–induced cell death, including that occurring in advanced atherosclerosis.

Materials and methods

Mice

C57BL/6J mice and *ob/ob* mice in the C57BL/6J background were purchased from The Jackson Laboratory. *Chop*$^{-/-}$ (*Ddit3*$^{-/-}$) mice were generated as previously described (Zinszner et al., 1998) and backcrossed for 10 generations into the C57BL/6J background. *Ero1a* mutant mice were generated from the embryonic stem cell line XST171 (Bay Genomics) with a disrupting insertion into the Ero1l locus. Chimeric mice were bred to C57BL/6J to generate heterozygous mutant F1 progeny that were intercrossed to generate female F2 siblings with divergent Ero1l genotypes from which macrophages were procured after methyl-BSA immunization as described in the next section.

Cells

Peritoneal macrophages from WT or mutant mice were harvested 3 d after i.p. injection of concanavalin A or 4 d after i.p. injection of methyl-BSA in mice that had previously been immunized with this antigen (Cook et al., 2003). Macrophages were harvested by peritoneal lavage with ice-cold PBS and maintained in DME containing 10% FBS and 20% L cell–conditioned medium. The medium was replaced every 24 h until the cells reached 80–90% confluency. Cholesterol loading was achieved by incubating the cells with 50 µg/ml acetyl–low density lipoprotein plus 10 µg/ml 58035 for the indicated times (DeVries-Seimon et al., 2005). The medium was changed every other day and immediately before treatments. MEFs from *Ero1a*$^{-/-}$ and littermate WT mice were prepared from 13.5-d embryos as described previously (Zinszner et al., 1998) and cultured in DME/10% FBS.

Calcium imaging

Macrophages cultured on 25-mm coverslips were placed in 35-mm dishes and loaded with 4 µM Fluo-3 acetoxymethyl ester (Invitrogen) and 0.08% Pluronic F-127 in HBSS at room temperature for 30 min. The cells were then washed twice with HBSS, incubated in HBSS for an additional 30 min, and then mounted on the stage of an inverted confocal microscope (Live5; Carl Zeiss, Inc.) equipped with a 40× objective. 250 µM sulphinpyrazone was included in all solutions to prevent excretion of the Fluo-3 by the macrophages. To trigger IICR, 10 µM ATP was added directly to the cell solution (Charest et al., 1985). In the experiments displayed in Fig. S1, 2 µM thapsigargin, a SERCA inhibitor, was added to assess ER calcium stores at the end of the experiment (Feng et al., 2003; Kim et al., 2008). Cells were excited using the 488-nm laser line, and images were acquired at 1-s intervals under time-lapse mode and subsequently analyzed using ImageJ (National Institutes of Health). The data are presented as a ratio of f_{max}/f_0, where f_{max} represents the maximum fluorescence intensity obtained with ATP stimulation and f_0 indicates the baseline fluorescence intensity. These data were quantified as either the increment in f_{max}/f_0 for the first peak or the area under the curve (AUC) for all peaks.

Apoptosis assay

Apoptosis was assayed by annexin V staining using the Vybrant Apoptosis Assay kit number 2 (Invitrogen; Yao and Tabas, 2000). At the end of the incubation period, the cells were gently washed once with PBS and then incubated for 15 min at room temperature with 110 µl of annexin V–binding buffer (25 mM Hepes, 140 mM NaCl, 1 mM EDTA, pH 7.4, and 0.1% BSA) containing 10 µl Alexa Fluor 488– or Alexa Fluor 594–conjugated annexin V. The staining mixture was removed and replaced with 110 µl of binding buffer. The cells were viewed immediately at room temperature with an inverted fluorescent microscope (IX-70; Olympus) equipped with filters appropriate for fluorescein (Alexa Fluor 488) or rhodamine (Alexa Fluor 594), and images were obtained with a charge-coupled device camera (CoolSNAP RS; Photometrics) equipped with imaging software from Roper Scientific. Three fields of ~700 cells per field were photographed for each condition, and the number of annexin V–positive cells in each field was counted and expressed as a percentage of the total number of cells.

Immunoblotting

Cell extracts were electrophoresed on 4–20% gradient SDS-PAGE gels (Bio-Rad Laboratories) and transferred to 0.22-µM nitrocellulose membranes. The membranes were blocked for 1 h at room temperature in Tris-buffered saline and 0.1% Tween 20 (TBST) containing 5% (wt/vol) nonfat milk. The membranes were then incubated with primary antibody in TBST containing 5% nonfat milk or BSA at 4°C overnight, followed by incubation with the appropriate secondary antibody coupled to horseradish peroxidase. Proteins were detected by ECL chemiluminescence (Thermo Fisher Scientific). Anti–murine ERO1-α antibody was purchased from Novus Biologicals; anti-CHOP antibody was purchased from Santa Cruz Biotechnology, Inc.; anti–β-actin and anti–phospho-Thr287-CaMKII antibodies were purchased from Millipore.

siRNA silencing of ERO1-α

siRNA sequences against murine ERO1-α were generated by QIAGEN. The target sequences were 5′-TAGGGCCTATTTATACTACAA-3′, 5′-CAGCTCTTCACTGGGAATAAA-3′, and 5′-TTGCTCGAAGTTCAAGTTTAA-3′ and are referred to in the text as ERO1-α siRNA #1, #2, and #3, respectively. A set of FlexiTube of siRNA against murine IP3R1 was purchased from QIAGEN (SI01079071, SI01079078, SI01079085, and SI01079092). The siRNA was transfected into macrophages grown to 50% confluency using Lipofectamine 2000 (Invitrogen) according to the manufacturer's instructions. A final mass of 50 pg siRNA was added to each well. After 4 h of transfection, the media were replaced, and 72 h later, the indicated experiments were conducted.

Adenoviral transduction

Adenoviruses containing the constructs for murine *Ero1a* or LacZ were made by Viraquest, Inc. Macrophages were infected with the virus at a MOI of 500 in medium containing 2% serum for 4 h, after which DME containing 10% FBS and 20% L cell-conditioned medium was added. Experiments were conducted 32 h later. Analysis of adeno-GFP expression indicated an infection rate of ~80%.

In vivo model of ER stress using i.v. tunicamycin

C57BL/6J mice and *Chop*$^{-/-}$ mice were injected i.p. with concanavalin A, and then 3 d later, the mice were given a single 20 µg/kg body weight i.v. injection of tunicamycin. After 16 h, peritoneal macrophages were collected, cultured on tissue culture dishes, and either probed for CHOP expression by immunoblot or assayed for IICR as described in Calcium imaging.

Statistics

Data are presented as mean ± SEM. For most of the bar graph data, $n = 3$ for each experimental group. However, for the bar graphs depicting f_{max}/f_0 data, n = ~30 per group. Analysis of variance followed by Tukey post-test (Prism 4 version 4.03; GraphPad Software, Inc.) was used to determine statistical significance among all groups.

Online supplemental material

Fig. S1 shows the thapsigargin-releasable ER calcium stores in response to ER stress and ERO1-α silencing. Fig. S2 shows the effect of ER stress on markers of the IRE1 and PERK branches of the UPR in WT versus *Ero1a*$^{-/-}$ cells. Online supplemental material is available at http://www.jcb.org/cgi/content/full/jcb.200904060/DC1.

We thank Drs. Edward Thorp, Dorien Schrijvers, and Connie Woo for helpful discussions during the course of this project.

This work was supported by National Institutes of Health (NIH) grants HL087123 and HL075662 and US Army Medical Research and Materiel Command grant W81XWH-06-1-0212 to I. Tabas and NIH grants DK47119 and ES08681 to D. Ron.

Submitted: 10 April 2009
Accepted: 16 August 2009

References

Boehning, D., R.L. Patterson, L. Sedaghat, N.O. Glebova, T. Kurosaki, and S.H. Snyder. 2003. Cytochrome *c* binds to inositol (1,4,5) trisphosphate receptors, amplifying calcium-dependent apoptosis. *Nat. Cell Biol.* 5:1051–1061. doi:10.1038/ncb1063

Chami, M., B. Oulès, G. Szabadkai, R. Tacine, R. Rizzuto, and P. Paterlini-Bréchot. 2008. Role of SERCA1 truncated isoform in the proapoptotic calcium transfer from ER to mitochondria during ER stress. *Mol. Cell*. 32:641–651. doi:10.1016/j.molcel.2008.11.014

Charest, R., P.F. Blackmore, and J.H. Exton. 1985. Characterization of responses of isolated rat hepatocytes to ATP and ADP. *J. Biol. Chem.* 260:15789–15794.

Cook, A.D., E.L. Braine, and J.A. Hamilton. 2003. The phenotype of inflammatory macrophages is stimulus dependent: implications for the nature of the inflammatory response. *J. Immunol.* 171:4816–4823.

Deniaud, A., O. Sharaf el dein, E. Maillier, D. Poncet, G. Kroemer, C. Lemaire, and C. Brenner. 2008. Endoplasmic reticulum stress induces calcium-dependent permeability transition, mitochondrial outer membrane permeabilization and apoptosis. *Oncogene*. 27:285–299. doi:10.1038/sj.onc.1210638

DeVries-Seimon, T., Y. Li, P.M. Yao, E. Stone, Y. Wang, R.J. Davis, R. Flavell, and I. Tabas. 2005. Cholesterol-induced macrophage apoptosis requires ER stress pathways and engagement of the type A scavenger receptor. *J. Cell Biol.* 171:61–73. doi:10.1083/jcb.200502078

Feng, B., P.M. Yao, Y. Li, C.M. Devlin, D. Zhang, H.P. Harding, M. Sweeney, J.X. Rong, G. Kuriakose, E.A. Fisher, et al. 2003. The endoplasmic reticulum is the site of cholesterol-induced cytotoxicity in macrophages. *Nat. Cell Biol.* 5:781–792. doi:10.1038/ncb1035

Grundy, S.M. 2004. Obesity, metabolic syndrome, and cardiovascular disease. *J. Clin. Endocrinol. Metab.* 89:2595–2600. doi:10.1210/jc.2004-0372

Hajnóczky, G., G. Csordás, S. Das, C. Garcia-Perez, M. Saotome, S. Sinha Roy, and M. Yi. 2006. Mitochondrial calcium signalling and cell death: approaches for assessing the role of mitochondrial Ca2+ uptake in apoptosis. *Cell Calcium*. 40:553–560. doi:10.1016/j.ceca.2006.08.016

Han, S., C.P. Liang, T. DeVries-Seimon, M. Ranalletta, C.L. Welch, K. Collins-Fletcher, D. Accili, I. Tabas, and A.R. Tall. 2006. Macrophage insulin receptor deficiency increases ER stress-induced apoptosis and necrotic core formation in advanced atherosclerotic lesions. *Cell Metab.* 3:257–266. doi:10.1016/j.cmet.2006.02.008

Higo, T., M. Hattori, T. Nakamura, T. Natsume, T. Michikawa, and K. Mikoshiba. 2005. Subtype-specific and ER lumenal environment-dependent regulation of inositol 1,4,5-trisphosphate receptor type 1 by ERp44. *Cell*. 120:85–98. doi:10.1016/j.cell.2004.11.048

Jayaraman, T., and A.R. Marks. 1997. T cells deficient in inositol 1,4,5-trisphosphate receptor are resistant to apoptosis. *Mol. Cell. Biol.* 17:3005–3012.

Kang, S., J. Kang, H. Kwon, D. Frueh, S.H. Yoo, G. Wagner, and S. Park. 2008. Effects of redox potential and Ca2+ on the inositol 1,4,5-trisphosphate receptor L3-1 loop region: implications for receptor regulation. *J. Biol. Chem.* 283:25567–25575. doi:10.1074/jbc.M803321200

Khan, A.A., M.J. Soloski, A.H. Sharp, G. Schilling, D.M. Sabatini, S.H. Li, C.A. Ross, and S.H. Snyder. 1996. Lymphocyte apoptosis: mediation by increased type 3 inositol 1,4,5-trisphosphate receptor. *Science*. 273:503–507. doi:10.1126/science.273.5274.503

Kim, I., W. Xu, and J.C. Reed. 2008. Cell death and endoplasmic reticulum stress: disease relevance and therapeutic opportunities. *Nat. Rev. Drug Discov.* 7:1013–1030. doi:10.1038/nrd2755

Li, Y., and P. Camacho. 2004. Ca^{2+}-dependent redox modulation of SERCA 2b by ERp57. *J. Cell Biol.* 164:35–46. doi:10.1083/jcb.200307010

Li, Y., M. Ge, L. Ciani, G. Kuriakose, E.J. Westover, M. Dura, D.F. Covey, J.H. Freed, F.R. Maxfield, J. Lytton, and I. Tabas. 2004. Enrichment of endoplasmic reticulum with cholesterol inhibits sarcoplasmic-endoplasmic reticulum calcium ATPase-2b activity in parallel with increased order of membrane lipids: implications for depletion of endoplasmic reticulum calcium stores and apoptosis in cholesterol-loaded macrophages. *J. Biol. Chem.* 279:37030–37039. doi:10.1074/jbc.M405195200

Lim, W.S., J.M. Timmins, T.A. Seimon, A. Sadler, F.D. Kolodgie, R. Virmani, and I. Tabas. 2008. Signal transducer and activator of transcription-1 is critical for apoptosis in macrophages subjected to endoplasmic reticulum stress in vitro and in advanced atherosclerotic lesions in vivo. *Circulation*. 117:940–951. doi:10.1161/CIRCULATIONAHA.107.711275

Malhotra, J.D., and R.J. Kaufman. 2007. The endoplasmic reticulum and the unfolded protein response. *Semin. Cell Dev. Biol.* 18:716–731. doi:10.1016/j.semcdb.2007.09.003

Marciniak, S.J., C.Y. Yun, S. Oyadomari, I. Novoa, Y. Zhang, R. Jungreis, K. Nagata, H.P. Harding, and D. Ron. 2004. CHOP induces death by promoting protein synthesis and oxidation in the stressed endoplasmic reticulum. *Genes Dev.* 18:3066–3077. doi:10.1101/gad.1250704

Nakagawa, T., H. Zhu, N. Morishima, E. Li, J. Xu, B.A. Yankner, and J. Yuan. 2000. Caspase-12 mediates endoplasmic-reticulum-specific apoptosis and cytotoxicity by amyloid-β. *Nature*. 403:98–103. doi:10.1038/47513

Narasimhan, K., I.N. Pessah, and D.J. Linden. 1998. Inositol-1,4,5-trisphosphate receptor-mediated Ca mobilization is not required for cerebellar long-term depression in reduced preparations. *J. Neurophysiol.* 80:2963–2974.

Nishitoh, H., A. Matsuzawa, K. Tobiume, K. Saegusa, K. Takeda, K. Inoue, S. Hori, A. Kakizuka, and H. Ichijo. 2002. ASK1 is essential for endoplasmic reticulum stress-induced neuronal cell death triggered by expanded polyglutamine repeats. *Genes Dev.* 16:1345–1355. doi:10.1101/gad.992302

Oyadomari, S., A. Koizumi, K. Takeda, T. Gotoh, S. Akira, E. Araki, and M. Mori. 2002. Targeted disruption of the Chop gene delays endoplasmic reticulum stress-mediated diabetes. *J. Clin. Invest.* 109:525–532.

Ozcan, U., Q. Cao, E. Yilmaz, A.H. Lee, N.N. Iwakoshi, E. Ozdelen, G. Tuncman, C. Görgün, L.H. Glimcher, and G.S. Hotamisligil. 2004. Endoplasmic reticulum stress links obesity, insulin action, and type 2 diabetes. *Science*. 306:457–461. doi:10.1126/science.1103160

Puthalakath, H., L.A. O'Reilly, P. Gunn, L. Lee, P.N. Kelly, N.D. Huntington, P.D. Hughes, E.M. Michalak, J. McKimm-Breschkin, N. Motoyama, et al. 2007. ER stress triggers apoptosis by activating BH3-only protein Bim. *Cell*. 129:1337–1349. doi:10.1016/j.cell.2007.04.027

Seimon, T., and I. Tabas. 2009. Mechanisms and consequences of macrophage apoptosis in atherosclerosis. *J. Lipid Res.* 50:S382–S387. doi:10.1194/jlr.R800032-JLR200

Seimon, T.A., A. Obstfeld, K.J. Moore, D.T. Golenbock, and I. Tabas. 2006. Combinatorial pattern recognition receptor signaling alters the balance of life and death in macrophages. *Proc. Natl. Acad. Sci. USA*. 103:19794–19799. doi:10.1073/pnas.0609671104

Senokuchi, T., C.P. Liang, T.A. Seimon, S. Han, M. Matsumoto, A.S. Banks, J.H. Paik, R.A. DePinho, D. Accili, I. Tabas, and A.R. Tall. 2008. Forkhead transcription factors (FoxOs) promote apoptosis of insulin-resistant macrophages during cholesterol-induced endoplasmic reticulum stress. *Diabetes*. 57:2967–2976. doi:10.2337/db08-0520

Song, B., D. Scheuner, D. Ron, S. Pennathur, and R.J. Kaufman. 2008. Chop deletion reduces oxidative stress, improves beta cell function, and promotes cell survival in multiple mouse models of diabetes. *J. Clin. Invest.* 118:3378–3389. doi:10.1172/JCI34587

Tajiri, S., S. Yano, M. Morioka, J. Kuratsu, M. Mori, and T. Gotoh. 2006. CHOP is involved in neuronal apoptosis induced by neurotrophic factor deprivation. *FEBS Lett.* 580:3462–3468. doi:10.1016/j.febslet.2006.05.021

Thorp, E., G. Li, T.A. Seimon, G. Kuriakose, D. Ron, and I. Tabas. 2009. Reduced apoptosis and plaque necrosis in advanced atherosclerotic lesions of *Apoe-/-* and *Ldlr-/-* mice lacking CHOP. *Cell Metab.* 9:474–481. doi:10.1016/j.cmet.2009.03.003

Timmins, J., L. Ozcan, T.A. Seimon, G. Li, C. Malagelada, J. Backs, T. Backs, R. Bassel-Duby, E.N. Olson, M.E. Anderson, and I. Tabas. 2009. Calcium/calmodulin-dependent protein kinase II links ER stress with Fas and mitochondrial apoptosis pathways. *J. Clin. Invest.* In press.

Watowich, S.S., and R.I. Morimoto. 1988. Complex regulation of heat shock- and glucose-responsive genes in human cells. *Mol. Cell. Biol.* 8:393–405.

Yao, P.M., and I. Tabas. 2000. Free cholesterol loading of macrophages induces apoptosis involving the fas pathway. *J. Biol. Chem.* 275:23807–23813. doi:10.1074/jbc.M002087200

Yao, P.M., and I. Tabas. 2001. Free cholesterol loading of macrophages is associated with widespread mitochondrial dysfunction and activation of the mitochondrial apoptosis pathway. *J. Biol. Chem.* 276:42468–42476. doi:10.1074/jbc.M101419200

Zinszner, H., M. Kuroda, X. Wang, N. Batchvarova, R.T. Lightfoot, H. Remotti, J.L. Stevens, and D. Ron. 1998. CHOP is implicated in programmed cell death in response to impaired function of the endoplasmic reticulum. *Genes Dev.* 12:982–995. doi:10.1101/gad.12.7.982